Experimental report on galvanostatic operation of electrolyte-supported stacks for high temperature electrolysis

Jérôme Aicart, Lionel Tallobre, Alexander Surrey, Denis Reynaud, Julie Mougin

A0808

Experimental Report on Galvanostatic Operation of Electrolyte-Supported Stacks for High Temperature Electrolysis

Jerome Aicart (1), Lionel Tallobre (1), Alexander Surrey (2), Denis Reynaud (1), Julie Mougin (1)
(1) Univ. Grenoble Alpes, CEA, Liten, DTCH, 38000 Grenoble, France
(2) Sunfire GmbH, 2 Gasanstaltstraße, D-01237 Dresden, Germany
Tel.: +33-43878-6744
jerome.aicart@cea.fr

Abstract

The field deployment of High Temperature Electrolyzers (HTE) has been accelerating in recent years under the promise of game-changing OPEX for Green Industrial Hydrogen (GrInHy) production. In the frame of the EU project GrInHy2.0, German company Sunfire has manufactured a 720 kW_{AC} HTE that produces a nominal H_2 flowrate of 200 $Nm^3.h^{-1}$. While drastic cost reduction has already been achieved, the Levelized Cost of Hydrogen (LCOH) is still largely controlled by stack manufacturing cost, stack replacement frequency, and therefore stack durability. In this view, one of the main objectives of the work package dedicated to stack testing is the demonstration of a 20,000 h lifetime.
A 30-cell electrolyte-supported stack manufactured by Sunfire was started mid-2020 at CEA-Liten on an in-house purpose-built test bench. It was operated for 4.5 kh, before a building-wide gas shutdown, consequence of an alarm-level H_2 detection unrelated to the test, led to significant damage of stack tightness and performances. Consequently, a replacement stack has been in operation since early 2021.
The present report details the testing equipment, the experimental conditions and procedures, and compares the performances and degradation rates recorded on the two stacks over their first 4.5 kh of operation. In addition, special attention is given to the de-ionized water quality over time. Indeed, periodic trace analyses at the part-per-trillion scale have been performed on 27 elements, and the results are reported. Finally, the evolutions of the building infrastructure based on the feedback received from these experiments is discussed.

Introduction

Interest in green hydrogen production via water electrolysis has been skyrocketing in recent years to replace natural gas in heavy-consuming industries or supply a slowly emerging market for mobility. Among the different technologies, Solid Oxide Electrolysis Cells (SOEC) operated between 700 and 850°C are particularly interesting due to their high DC power-to-H_2 efficiencies, promising potential game-changing OPEX for Green Industrial Hydrogen (GrInHy) production.
Started in 2019, one of the objective of the FCHJU GrInHy2.0 project is the demonstration of a 20,000 h lifetime at Sunfire's (GmbH) stack level, a major step towards reducing the high current costs of implementation of the technology. For this purpose, a dedicated purpose-built test bench has been commissioned at CEA, and a first experiment was carried out over the second half of 2020. An unfortunate series of events precipitated the stack End-of-Life (EoL), and a second stack has been in operation since March 2021.
The present report gathers experimental results collected on both stacks and compares their first 4,500 h of operation. Performance and low degradation rates are highlighted. A special attention was given to de-ionized water quality over time, as well as the evolution of the testing overall infrastructure stemming from these results.

1. Experiments

1.1. Cells and Stack Design

The Sunfire stack design, as described in previous publications [1–3], comprises 30 electrolyte-supported cells (ESC) with Ni-GDC H_2 electrode, 3YSZ electrolyte, and LSCF-GDC oxygen electrode. The stack is further characterized by a metal cassette interconnector out of Crofer 22 APU with a MCF coating at the oxygen side.
In S1, four slightly different cell variants were used, which included promising advanced electrodes. In Stack 2 only the best variant was implemented. Furthermore, Stack 2 has been optimized by continuously improving quality assurance processes during the manufacturing.

1.2. Testing Equipment

A dedicated, purpose-built test bench was designed and commissioned for this project, as summarized in Figure 1. Inlet gas flowrates were controlled using thermal mass flow controllers (Brooks, 5850S), while steam is generated with an in-house engineered direct evaporator. A heating wire placed between the steam generator and the furnace prevented condensation. The liquid flowrate was controlled using a Coriolis mass flow controller (Brooks, Quantim), fed from the building own de-ionized network. Due to the long test duration targeted, special attention was given in the bench design to securing the stack when failures happen. Among many safety features, in case of a bench-wide loss of power, the stack would be supplied with nominal flowrates of 4 vol.% H_2 balance N_2 on the H_2 side and air on the O_2 side through a combination of normally open valves and float meters. Another safety implementation was to monitor the power consumption of the steam generator. Indeed, regulation being done here on liquid water, a sudden failure of the heating element used for vaporization would be invisible to the Programmable Logic Controller (PLC) until steam starvation occurs. An alarm was therefore created based on a minimum power consumption, and passing under that threshold would trigger a transition towards hot stand-by conditions.

Gas connections to the stack were achieved using an adapter plate (Sunfire GmbH), located in a top-down furnace divided in three distinct thermal zones individually controlled: bottom, middle and top. The bottom part of the furnace was regulated so that the inlet gases, after going through several preheating loops, reached the stack at (or close to) the stack temperature. All high temperature inlet pipes were treated to prevent chromium (Cr) evaporation and limit Solid Oxide Cell (SOC) contamination. The middle and top parts of the furnace were regulated to get a near uniform stack temperature field at Open Circuit Voltage (OCV) and compensate for thermal losses. Airflow was directed through the open air manifold of the stack using an external housing around the stack (Sunfire GmbH). However, no outlet air could be collected and measured, most likely due to pressure drops through the outlet flowmeter being too high compared to the sealing ability of the housing. An airflow sweeping the furnace was maintained at all time for safety reasons, insuring that any H_2 leakage would burn immediately and that the O_2 would be replaced, effectively preventing any ATEX formation. The furnace airflow also allowed diluting the O_2 produced electrochemically. At the bench outlet, both fuel and air lines went through a cooling heat exchanger fed from the building cooling water network, a separation stage to evacuate condensates to the drain, and a flow measurement before being vented out.
DC current was generated by a 6 kW_{DC} power supply (Micronics), and connections to the stack were managed using proprietary high temperature conductors. All 30-cell voltages were individually recorded. Six type-K thermocouples were inserted at various depth in the center of stack along the airflow channels, in addition to measuring the temperatures of inlets and outlets at the adapter plate/stack interface. Stack inlet and outlet pressures were measured outside of the furnace, and the pressure difference at the inlet was monitored.

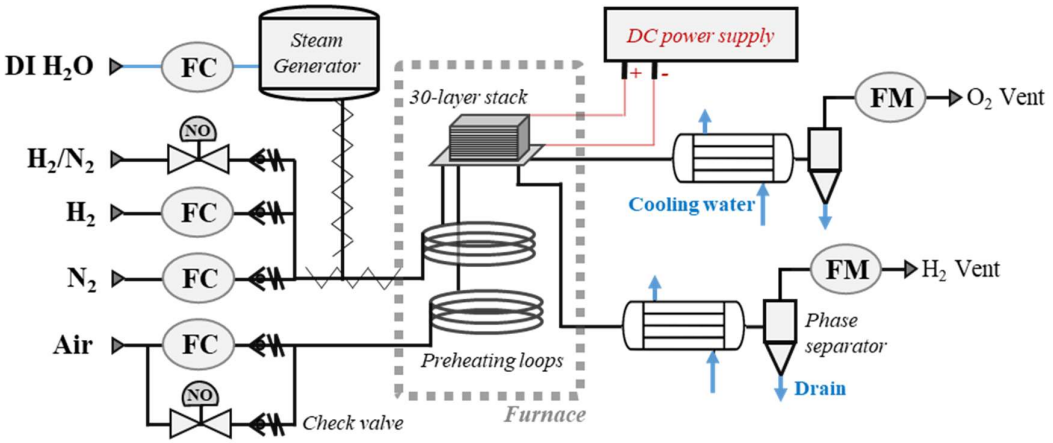

Figure 1 : Overview of the test bench. FC: flow controller, FM: flow meter.

1.3.Protocol and Operational Strategy

The chronological testing sequence includes startup procedures, initial performance mapping, followed by galvanostatic operation, with a targeted duration of 20 kh. Temperature ramps were performed at a rate of 3°C.min^{-1} in 4 vol.% H_2 balance N_2 on the H_2 side up to 600°C, after which the amount of H_2 was increased. Oxygen electrodes were fed with air. All electrolysis measurements were carried out in 90/10 vol.% H_2O/H_2 inlet composition. Whenever applicable, the steam conversion (SC) was set to 70%. Current ramp rate was set to 5 A.min^{-1} below 50 A, and 1.5 A.min^{-1} above. Finally, degradation was compensated by increasing stack temperature and maintain thermoneutral operation. Additional details on the overall experimental protocol can be found in the corresponding public deliverable, available on GrInHy2.0 website [4].

2. Results

2.1.Initial Electrochemical Tightness Test

The Electrochemical Tightness Test (ETT) consisted in cutting off all inlet gases, from dry stand-by conditions (H_2 balance N_2), and recording the rate of OCV decrease over time. The faster the decrease, the larger the leak. In addition, depending on whether all or individual cell voltages are limiting the test can yield information on the localization of the leak. More details on the test can be found in Grinhy2.0 public deliverable "D3.1 Definition of long-term stack test protocol", available from the project's website [5].
The initial results of this test carried out on Stack n°1 are given in Figure 2. The initial stack tightness was satisfactory, as the test ended due the targeted duration being reached (20 min), as opposed to a limiting cell hitting a lower threshold (1 V). Nevertheless, U30 was recorded being slightly below the rest of the cell voltages, while still remaining above 1 V during the complete duration of the test.

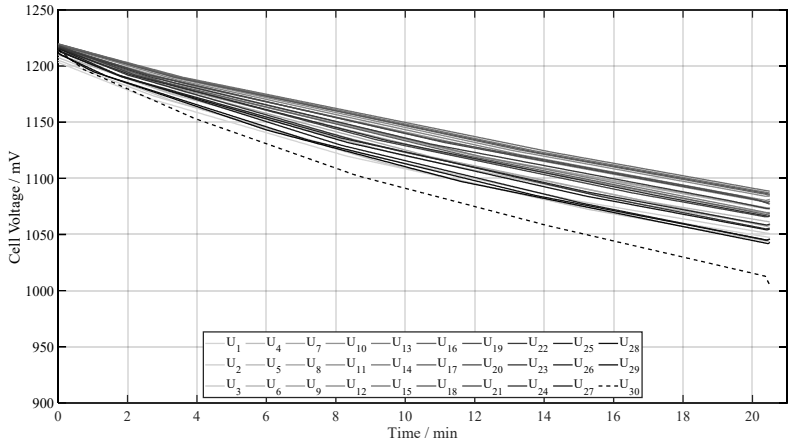

Figure 2 : Cell voltages evolution during the initial electrochemical tightness test carried out on Stack n°1. During the test, all inlet gas flowrates are cut off.

2.2.Initial Performances

Following the ETT, preliminary stack assessment involved recording the initial performances over a designated range of temperature. From a stable and homogeneous thermal state at OCV, checked using all 10 thermocouples installed either in the stack or in the gas manifold, current and inlet flowrates were incrementally adjusted to satisfy simultaneously (i) average cell voltage at (or near) the isothermal voltage, (ii) 70% steam conversion (SC), and (iii) temperatures under load equal (or very close) to that at OCV. For simplicity, such current will be described as the thermoneutral current, and the overall conditions by THN70 (thermoneutral, 70% SC).
The initial performance results of both stacks are presented in Figure 3. They are strikingly similar over the complete range of temperatures, likely due to a robust manufacturing process. The performances span from about -0.35 A.cm^{-2} at 780°C to approximately -0.6 A.cm^{-2} at 850°C, while -0.65 A.cm^{-2} was initially targeted for the durability test. In this last condition, the Beginning-of-Life (BoL) temperature was very close to the maximum acceptable temperature, 860°C. Consequently, it was decided to keep instead the targeted BoL temperature around 830°C, setting the current density in THN70 conditions at -0.52 A.cm^{-2}.

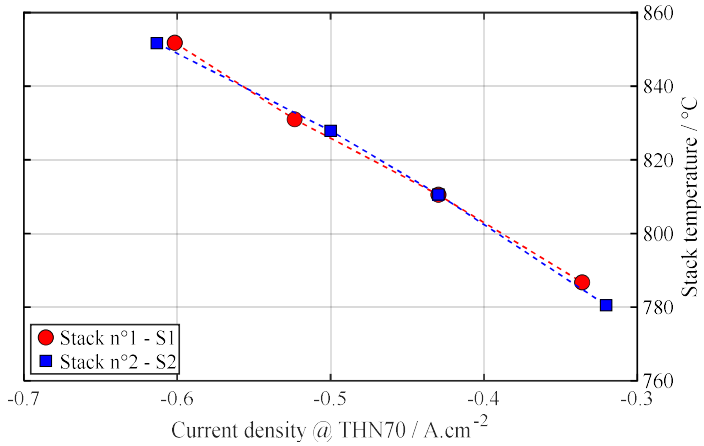

Figure 3 : Temperature dependence of initial current densities near isothermal voltage and at 70% steam conversion for both stacks tested.

2.3.Time Evolutions and Notable Events

2.3.1. Overview

Following Figure 4 displays the time evolutions of stack current, voltage and power, cell voltages, as well as minimum, average and maximum temperatures taken from the six type-K thermocouples installed in both Stack 1 (S1, left) and Stack 2 (S2, right). The 700 h gap in data for S2 corresponds to the annual technical shutdown of the building, used to check safety features and upgrade infrastructure. The voltage sensors for cell 2 of S2 broke during mounting, so both U_{2*} and U_{3*} relate to $(U_2+U_3)\div 2$. Figure 5 displays the evolutions of stack ASR and temperature over the time spent in operation.

Brief comparison of the stacks behavior leads to striking differences. First, cell 30 of S1 experienced a much enhanced degradation rate compared to the others. Explanations and details are given in the following paragraph. Cell voltage scattering is much more pronounced on S1 as well, likely explained by the different types of cells incorporated in the stack. For example, after 1 kh of operation, voltage scattering was 130 mV for S1 (120 mV excluding U30), and 35 mV for S2. Finally, strong differences were recorded for the rates of temperature evolution over time, akin to degradation due to the operational strategy. Overall, S1 evolved at a rate of +4.2°C.kh^{-1}, while only +2.7°C.kh^{-1} was recorded with S2. The corresponding ASR degradation rates for S1 and S2 were 22 and 13 mOhm.cm^2.kh^{-1}. Details on ASR calculations can be found in reference [6]. The plotted ASR values are all referenced to a temperature of 860°C using the known ASR(T) relationship, whereby the temperature increase of the stack is taken into account for the derived degradation.

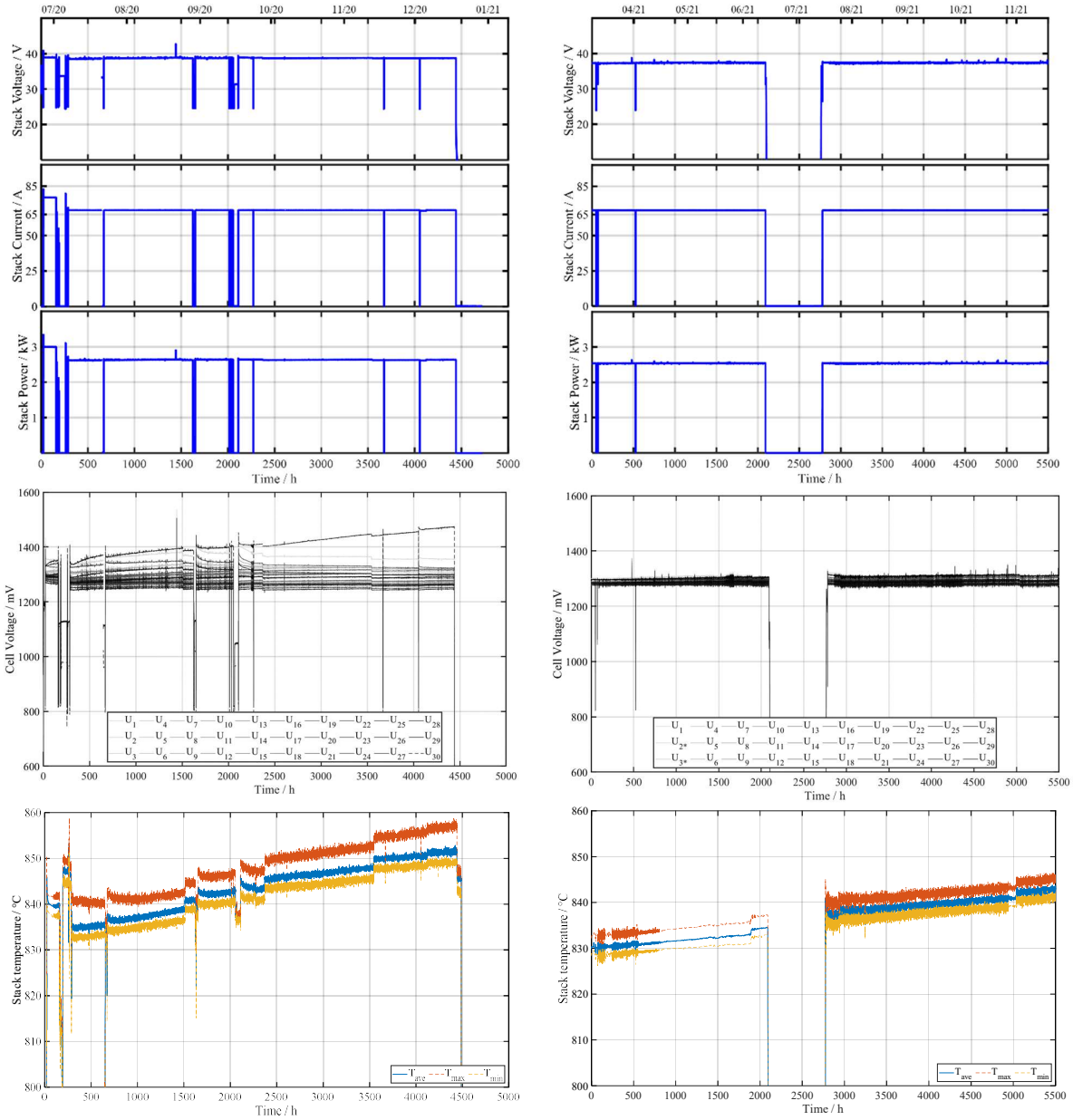

Figure 4 : Time evolutions of stack voltage, current and power, individual cell voltages and stack temperatures for Stack 1 (S1, left) and Stack 2 (S2, right).

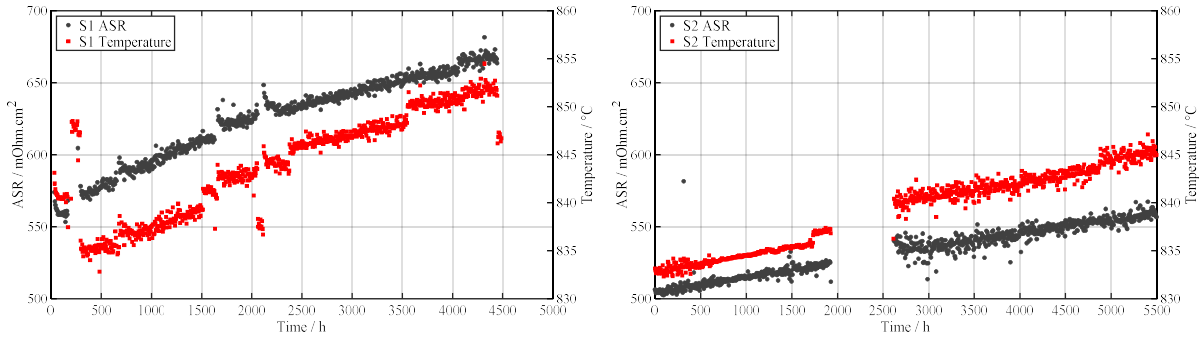

Figure 5 : Stack ASR and maximum temperature depending on time spent in operation at high temperature.

2.3.2. Localized Loss of Tightness (S1)

After approximately 200 h at high temperature, S1 suffered a sudden loss of tightness localized on top cell 30, later attributed to stack manufacturing defect. The event occurred at OCV after switching gas conditions from 90/10 vol.% H_2O/H_2 to dry N_2/H_2 for the night following the measurement of initial performances, as shown in Figure 6, where a dramatic drop in OCV is indeed observed. One of the thermocouple located inside the stack was positioned on cell 30, and picked up an increase of temperature compared to the other stack thermocouples, which persisted until the end of the test. The damaged seal led to a much increased degradation rate for this cell, as evidenced by its voltage steadily increasing over time despite increasing stack temperature. In the end, this ended up limiting the overall stack performances and lifetime. Indeed, after about 4.5 kh of operation, the corresponding temperature sensor was getting close to the maximum allowed operating temperature of 860°C, approximately 8°C hotter than the stack average temperature. Another few hundred hours of operation would have led to periodically decrease the current density to maintain temperature and compensate degradation.

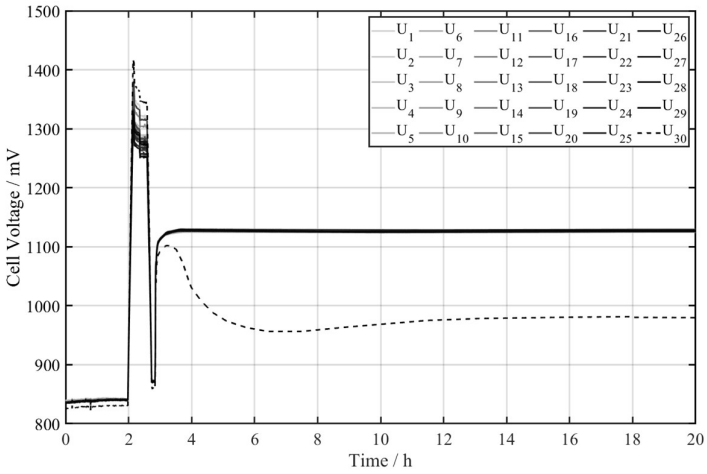

Figure 6 : Time evolution of S1 cell voltages during the loss of tightness on cell 30.

(0-3h: 90/10 vol.% H_2O/H_2
3-20h: 95/5 vol.% N_2/H_2
2-3h: polarized)

2.3.3. Current Ramp Rate & Thermal Consequences

Figure 7 (left) shows the temperature evolutions of the six thermocouples located in the stack during an early power ramp up on S1. Going from OCV to the (near) thermoneutral voltage lasted approximately 30 min according to the ramp rate of the testing protocol (0 to 77 A), during which stack operation was entirely endothermal [7,8]. While the temperature sensors were only separated by a few centimeters, a maximum temperature difference of approximately 29°C was recorded between temperatures at OCV (about 852°C) and during the transient state (minimum of 823°C). These results highlight the strong temperature gradients that can appear when the stack is not operated at or around the thermoneutral voltage.

After about 1,700 h of operation, the “high cell voltage alarm” of S1 was triggered a few times during power ramps. More peculiarly, one of such events happened during a current ramp down, as shown in Figure 7 (right). The cells then incriminated were located in 1st, 11th and 20th positions, notably adjacent to the thicker elements of the stack: end plates or thick interconnects every 10 cells to provide additional mechanical structure. It was then hypothesized that the thermal gradient during power ramps led to slight deformations of the thicker elements, inducing partial loss of electrical contact with the adjacent cells. Consequently, the current ramp rate was increased to 100 $A.min^{-1}$, yielding excellent results

and circumventing any of the previously observed high voltage limitations. This fast current control strategy was adopted for all subsequent current ramps for S1 and S2, and has since been successfully implemented in other works to avoid thermal gradients [9,10].

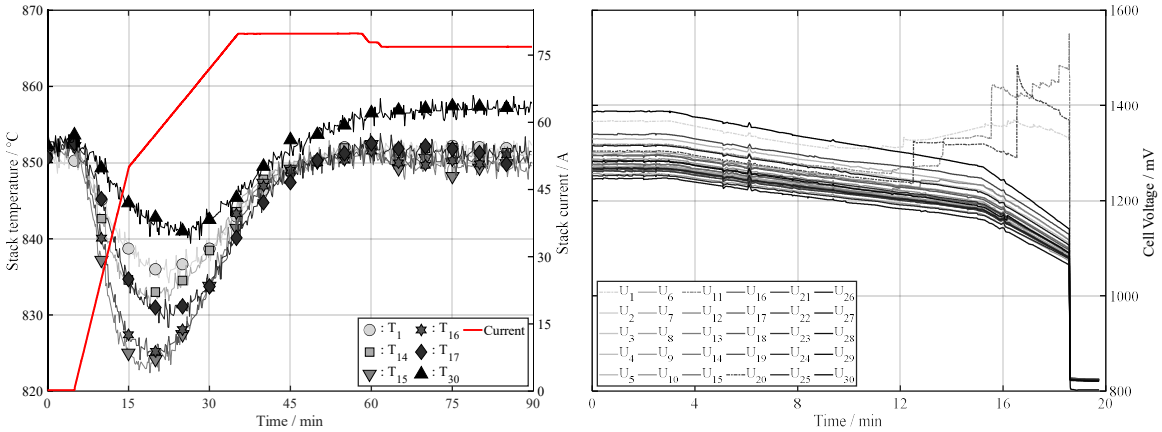

Figure 7: (left) time evolution of stack temperature during an early current ramp-up, (right) cell voltage evolution during a later current ramp-down, both for S1.

2.3.4. Series of Events Leading to S1 End-of-Life

On December 27th 2020, during the annual closing week at CEA, a faulty safety release valve on the H_2 network of the building-adjacent gas park led to an alarm-level detection and initiated a building-wide gas cutoff. After H_2 was depleted from the laboratory feed pipes, the stack was operating under 100% steam. While this should not have been an issue, the absence of H_2 flowrate and counter pressure led to some of the inlet steam to back travel up the H_2 pipe (Figure 1), lowering temporarily the actual supply to the stack. Unfortunately, cell 30 already exhibiting a high voltage, this was just the push necessary to cross the alarm level threshold on cell voltages, triggering a cutoff of the DC power supply. Without H_2 supply nor current, the stack was left at OCV and 100% steam for two days and therefore underwent a redox cycle, before being brought back to room temperature during a dedicated technical visit on site. Consequently, tightness and performances were severely affected, precipitating the end of the test.

2.3.5. Deionized Water Analyses

Throughout the GrInHy2.0 project, special attention was given to the quality of the deionized (DI) water. The test bench is fed by an ultrapure water network. The last step of purification is performed by a mixed bed demineralizer that contains ion exchange resins.
Initial quantifications of the silica content were later on completed with measurements on 26 different species. The method quantification limits ranged from 5 to 100 parts per trillion (ppt). Figure 8 and Figure 9 show the results of these analyses.

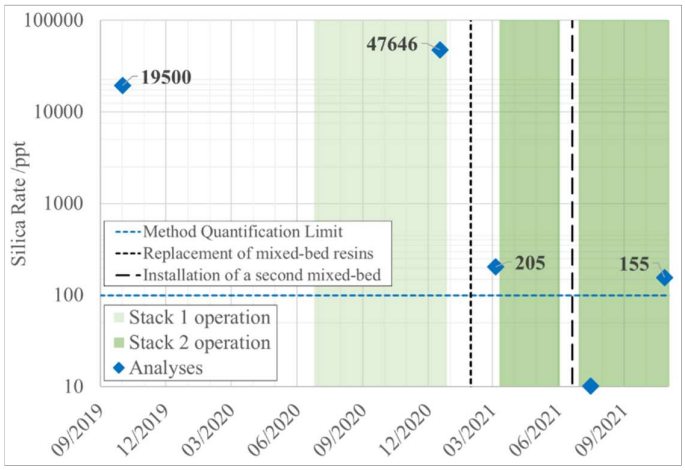

Figure 8: Chronology and evolution of dissolved silica in deionized water.

Figure 7 shows a significant initial concentration of dissolved silica (19.5 ppb), yet rising during S1 operation to approximately 48 ppb. This was caused by a faulty monitoring of the deionized water conductivity and the resin of the mixed bed demineraliser had to be replaced. This could be done just after S1 EoL. Subsequent analyses showcased very low concentrations of impurities. For example, Stack 2 was started with a dissolved silica rate lower than 1 ppb in the deionized water. This concentration was still lower than 1 ppb after 4,500 hours of Stack 2 operation (155 ppt).

In addition to the dissolved SiO_2 analyses, quantifications were carried out on 26 other elements throughout Stack 2 lifetime. Figure 8 shows the full set of results corresponding to the analyses done at the same time of the SiO_2 analysis of March 2021 (Stack 2 BoL) and July 2021 (around 2,600 hours of operation). In the former, 14 elements were detected, all with rates of around 1 ppb or less. In the latter, 6 elements were then identified, all with concentrations lower than 100 ppt. This last analysis was done after the installation of a second mixed-bed demineraliser in series with the first one.

These results highlight the substantial DI water quality produced in the laboratory. The distribution network from the production unit to test benches is also worthy of note, since the water purity is sustained. In addition to improving the purification process, the installation of a second mixed bed now allows replacement of the resins without stopping the DI water production.

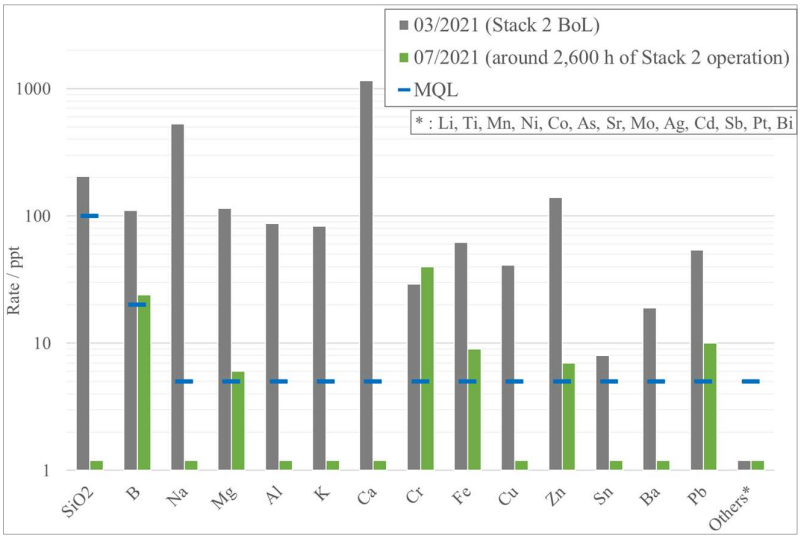

Figure 9: Rate evolutions of 26 elements & SiO_2 in deionized water collected at the bench inlet (MQL: Method Quantification Limits).

3. Discussion

3.1. Stack Comparison

There was a larger variation of cells mixed in S1 and the four different variants showed slightly different degradation rates. In Stack 2 only the best variant was tested, showing an even lower degradation compared to S1 (13 vs. 16 mOhm.cm².kh^{-1} on average, and 10 vs. 14 mOhm.cm².kh^{-1} for minimum values). This may be attributed to a lower contamination level during the test of Stack 2 coming from the DI water or the brand new test bench components, which passivated over time. The degradation of S1 is clearly decreasing over time and not as linear as of Stack 2 (see Figure 5), which supports this explanation.
Furthermore, a continuously ongoing stabilization of the manufacturing processes at Sunfire can be another reason for the reduced degradation since the cells for Stack 2 were produced later than the cells of S1. The variation in degradation of Stack 2 is also very small, from 10 to 17 mOhm.cm².kh^{-1}, demonstrating a very reproducible cell production process. Small differences in the calculated degradations also stem from measurement uncertainties and a slightly changing temperature profile across the stack.
The loss of tightness of S1 localized on the top cell 30 was due to a manufacturing defect in the glass sealing, which occurred on R&D stacks only. This issue was solved for Stack 2 showing a perfect tightness for the whole testing time so far.
For both solid oxide stacks, due to the sustained operation near the thermoneutral voltage, the energy cost of hydrogen production (DC power-to-H_2) was consequently near-constant at approximately 35 kWh.kgH_2^{-1}. This result is unsurprisingly consistent with previously reported data [9]. Another consequence of this operational strategy is that no loss of H_2 production was recorded throughout the entire testing sequences.

3.2. Infrastructure Evolutions

Following the destruction of S1, several infrastructure upgrades were implemented either right away or during the following annual technical shutdown of the building. From a gas perspective, the H_2 network and several of its components were modified to suppress the need for safety release valves altogether. In addition, the N_2/H_2 safety gas network, along with the corresponding control valves automation and overall safety matrix were modified so that the building would remain supplied in the event of a gas alarm originating from the gas park. Regarding the DI water impurity levels, as previously stated, a second mixed bed (the final stage of ultra-purification) was installed, along with a series of manual valves allowing bypass and maintenance without interruption of the supply. Finally, tracking of the in-line conductivity measurement has now been automated, and a dedicated service contract has been signed for periodic trace element analyses.

4. Conclusions

In the frame of the FCHJU project GrInHy2.0, the main objective of the work package dedicated to stack testing in a laboratory environment is the experimental demonstration at CEA of a 20,000-hour lifetime on Sunfire GmbH state-of-the-art solid oxide stack.
A first 30-cell stack, comprising several cell variants, was started in 2020. A leak quickly appeared, leading to an accelerated degradation rate on the impacted top cell, and later attributed to a manufacturing defect. Strong thermal gradients and suspected subsequent loss of electrical contact led to the successful implementation of a fast current control strategy. After 4.5 kh of operation, a malfunction of one of the building safety component led to the stack destruction. Consequently, a new experiment was started with a second stack only comprising the best cell variant. Due to the operational strategy of compensating degradation by increasing the temperature and maintaining thermoneutral conditions, no production loss was evidenced throughout the entire testing sequences.
The overall behavior of both stacks was quite different. The rate of temperature increase for S1 was slowing down with time and higher temperature, mainly caused by a degressive degradation, while that of S2 behaved much more linearly with a lower degradation rate. These differences might be attributed to (i) a more robust manufacturing process of S2, (ii) a decrease of impurity levels released by the test bench as it passivated, or (iii) a decrease of impurities in the deionized (DI) water used to produce steam. At stack level, degradation rates recorded were 16 and 13 $mOhm.cm^2.kh^{-1}$ for S1 and S2, respectively. To the best of the authors knowledge, this is among the lowest, if not the lowest ASR degradation rate of published SOEC stack tests in comparable conditions. At the time of writing this report, S2 has past 9,000 hours of operation with the same low degradation rate.
Punctual analyses of the DI water purity were carried out throughout the different testing sequences. While initial results allowed identifying that the last purification step was saturated, replacement of the resins of the mixed bed and further strengthening of the process allowed S2 to be operated with DI water of substantial quality.
Finally, feedback stemming from these experiments led to several modification of the surrounding infrastructure to reinforce the overall resilience to shutdowns and malfunctions, more likely to happen as the test durations increase.

Acknowledgments

This work has received funding from the Fuel Cells and Hydrogen 2 Joint Undertaking (JU) (now Clean Hydrogen Partnership) under grant agreement No 826350. This Joint Undertaking receives support from the European Union's Horizon 2020 Research and Innovation programme, Hydrogen Europe and Hydrogen Europe Reasearch.

References

[1] Lang M, Raab S, Lemcke MS, Bohn C, Pysik M. Long Term Behavior of Solid Oxide Electrolyser (SOEC) Stacks. ECS Trans 2019;91:2713–25. doi:10.1149/09101.2713ecst.
[2] Riedel M, Heddrich MP, Friedrich KA. Analysis of pressurized operation of 10 layer solid oxide electrolysis stacks. Int J Hydrog Energy 2019;44:4570–81. doi:10.1016/j.ijhydene.2018.12.168.

[3] Preininger M, Stoeckl B, Subotić V, Mittmann F, Hochenauer C. Performance of a ten-layer reversible Solid Oxide Cell stack (rSOC) under transient operation for autonomous application. Appl Energy 2019;254:113695. doi:10.1016/j.apenergy.2019.113695.
[4] GrInHy2.0 project website n.d. https://www.green-industrial-hydrogen.com/.
[5] MultiplHY project website n.d. https://https://multiplhy-project.eu/.
[6] Kusnezoff M, Beckert W, Trofimenko N, Jacobs B, Dosch C, Megel S, et al. Electrochemical MEA Characterization: Area Specific Resistance Corrected to Fuel Utilization as Universal Characteristic for Cell Performance. ECS Trans 2015;68:2555–63. doi:10.1149/06801.2555ecst.
[7] Laurencin J, Kane D, Delette G, Deseure J, Lefebvre-Joud F. Modelling of solid oxide steam electrolyser: Impact of the operating conditions on hydrogen production. J Power Sources 2011;196:2080–93. doi:10.1016/j.jpowsour.2010.09.054.
[8] Aicart J. Modeling and Experimental Validation of Steam and Carbon Dioxide Co-Electrolysis at High Temperature. PhD Thesis. Grenoble-Alpes, 2014.
[9] Aicart J, Wuillemin Z, Gervasoni B, Reynaud D, Waeber F, Beetschen C, et al. Performance evaluation of a 4-stack solid oxide module in electrolysis mode. Int J Hydrog Energy 2022;47:3568–79. doi:10.1016/j.ijhydene.2021.11.056.
[10] Aicart J, Surrey A, Champelovier L, Henault K, Geipel C, Posdziech O, et al. Benchmark Study of Performances and Durability between Different Stack Technologies for High Temperature Electrolysis. 15th Eur. SOFC SOE Forum, vol. A0804, Lucerne, Switzerland: 2022, p. 1–13.

Keywords: *EFCF 2022, Solid Oxide Technologies, SOC, Electrolysers, SOE, electrolyte-supported, durability, performances, GrInHy2.0*